

# A quantum Poisson solver implementable on NISQ devices

Shengbin Wang<sup>1,4</sup>, Zhimin Wang<sup>1,3,4</sup>, Wendong Li<sup>1</sup>, Lixin Fan<sup>1</sup>, Guolong Cui<sup>1</sup>, Zhiqiang Wei<sup>2</sup> and Yongjian Gu<sup>1,3</sup>

<sup>1</sup> Department of Physics, College of Information Science and Engineering, Ocean University of China, Qingdao 266100, China

<sup>2</sup> Department of Computer Science and Technology, College of Information Science and Engineering, Ocean University of China, Qingdao 266100, China

<sup>3</sup> Author to whom any correspondence should be addressed,  
E-mail: wangzhimin@ouc.edu.cn; guyj@ouc.edu.cn

<sup>4</sup> These authors contributed equally: Shengbin Wang, Zhimin Wang

## ABSTRACT

Solving differential equations is one of the most compelling applications of quantum computing. Most existing quantum algorithms addressing general ordinary and partial differential equations are thought to be too expensive to execute successfully on Noisy Intermediate-Scale Quantum (NISQ) devices. Here we propose a compact quantum algorithm for solving one-dimensional Poisson equation based on the simple  $R_y$  rotation. The major operations are performed on probability amplitudes. Therefore, the present algorithm avoids the need to do phase estimation, Hamiltonian simulation and arithmetic. The solution error comes only from the finite difference approximation of the Poisson equation. Our quantum Poisson solver (QPS) has gate-complexity of  $3n$  in qubits and  $5/3n^3$  in one- and two-qubit gates, where  $n$  is the logarithmic of the dimension of the linear system of equations. In terms of solution error  $\varepsilon$ , the complexity is  $\log(1/\varepsilon)$  in qubits and  $\text{poly}(\log(1/\varepsilon))$  in operations, which is consistent with the best known results. The present QPS may represent a potential application on NISQ devices.

## 1. INTRODUCTION

Quantum computing is capable of solving problems efficiently which are intractable for classical computing. Since the discovery of Shor's factoring algorithm [1], quantum algorithms demonstrating advantages over classical methods have been developed for a substantial variety of tasks [2]. One of the most compelling applications is for solving differential equations which is the main task in high-performance scientific computing.

A series of quantum algorithms for solving ordinary and partial differential equations (ODEs and PDEs) have been developed, which promise an exponential speed-up over classical algorithms in the dimension of equations and solution errors [3-9]. The main idea of these algorithms is that encoding the differential equations as a linear system, and solving it by Quantum Linear Systems Algorithm (QLSA) [10-12] or Hamiltonian simulation [13,14]. These algorithms are general methods for a class of differential equations. They are considered to be out of reach without large-scale fault-tolerant quantum computers.

In present paper, we focus on the problem of solving the one-dimensional Poisson

equation by discretizing it into a linear system of equations using the finite difference approximation. The Poisson equation, usually expressed as  $\nabla^2\varphi = f$ , is a widely used PDE across many areas of physics and engineering [15]. Many quantum algorithms are proposed to solve the general Poisson equation [7,9,16-18]. Compared with them, the present algorithm has a much lower gate-complexity. It would be implementable on Noisy Intermediate-Scale Quantum (NISQ) devices.

The inspiration of our method is from the observation that the eigenvalues of the discretized matrix of the Poisson equation are square of sine values and sine values can be prepared as the probability amplitudes easily by  $R_y$  rotation. The QLSA is actually to produce a quantum state with probability amplitudes being the reciprocals of eigenvalues. There should exist a simple way of accomplishing it by operating  $R_y$  rotation only. That is, all the transformations are performed on the probability amplitude. With such a way, we could eliminate the need for phase estimation, Hamiltonian simulation [13,14] and quantum arithmetic [19-21], which are the major contributors to the gate-complexity.

It is intriguing that the above inspiration is realized quite naturally from the fact that the product of all eigenvalues of the discretized matrix equals constant. The product is a sine formula which is derived from the study of Cartan matrix in Lie algebra [22]. Benefiting from the  $R_y$  rotation and the sine formula, we establish an efficient quantum Poisson solver (QPS) with the complexity of  $3n$  in qubits and  $5/3n^3$  in one- and two-qubit gates, where  $n$  is the logarithmic of the dimension of the linear system. With the rapid developments of quantum hardware and techniques [23-26], our QPS should be able to be executed successfully on NISQ devices.

This paper is organized as follows. In Section 2, we provide an overview of the problem we address and the main idea of our algorithm. In Section 3, we describe the quantum algorithm and circuit in detail, including the implements of each module. The gate-complexity, depth and error analysis of the algorithm are discussed in Section 4. Section 5 shows the demonstration results of the present circuits on a quantum virtual system. Finally, conclusions are discussed in Section 6.

## 2. OVERVIEW OF THE PROBLEM AND METHOD

The problem we address is solving the one-dimensional Poisson equation with Dirichlet boundary conditions, which can be described as

$$-\frac{d^2v(x)}{dx^2} = b(x), x \in (0,1), \quad (1)$$

$$v(0) = v(1) = 0.$$

The  $b(x)$  is a given smooth function representing, say, charge distribution in electrostatics problems or velocity distribution in fluid dynamics problems, and  $v(x)$  is the unknown to solve.

We choose the simple central difference approximation to discretize the second-order derivative, then Eq. (1) in the finite difference form is,

$$\begin{aligned} h^{-2}(-v_{i-1} + 2v_i - v_{i+1}) &= b_i + \varepsilon_i, i = 1, 2, \dots, N-1, \\ v_0 = v_N &= 0. \end{aligned} \quad (2)$$

The number of discrete points is  $N+1$  and the mesh size  $h$  equals to  $1/N$ . The  $\varepsilon_i$  is the truncation error induced by the finite difference approximation which can be shown to be  $O(h^2 \cdot \|d^4 v/dx^4\|_\infty)$  [27]. When  $b(x)$  is smooth enough, the norm of the fourth derivative is bounded uniformly independent of  $h$ . It is worth noting that this truncation error is the only error of the solution solved by our algorithm. So the final solution error is  $\varepsilon = h^2 = 1/N^2$ , which will be discussed subsequently.

Ignoring the truncation error in Eq. (2), now the problem of solving one-dimensional Poisson equation transfers into solving a linear system of equations as follows,

$$A\vec{v} = \vec{b} \Rightarrow h^{-2} \begin{pmatrix} 2 & -1 & & 0 \\ -1 & \ddots & \ddots & \\ & \ddots & \ddots & -1 \\ 0 & & -1 & 2 \end{pmatrix} \cdot \begin{pmatrix} v_1 \\ v_2 \\ \vdots \\ v_{N-1} \end{pmatrix} = \begin{pmatrix} b_1 \\ b_2 \\ \vdots \\ b_{N-1} \end{pmatrix}. \quad (3)$$

Matrix  $A$  is a well-studied tridiagonal Toeplitz matrix. The eigenvectors and corresponding eigenvalues are  $u_j(k) = \sqrt{2/N} \sin(j\pi k/N)$  and  $\lambda_j = 4N^2 \sin^2(j\pi/2N)$ , respectively [27]. Such a linear system of equations can be, of course, solved using the standard QLSA as done in Refs. [16,18]. The solution state  $|v\rangle$  would be expressed as

$$|v\rangle = A^{-1}|b\rangle = \left(\sum_j \frac{1}{\lambda_j} |u_j\rangle\langle u_j|\right) \cdot \left(\sum_{j'} \beta_{j'} |u_{j'}\rangle\right) = \sum_j \beta_j \frac{1}{\lambda_j} |u_j\rangle. \quad (4)$$

In order to produce such state, the HHL algorithm first estimates the eigenvalue  $\lambda_j$  for each eigenvector  $u_j$  through phase estimation, then calculates the reciprocal of  $\lambda_j$  and converts it from binary string to probability amplitude.

Here we propose a much simple way of producing the solution state based mainly on  $R_y$  rotations. The sine formula derived from Cartan matrix [22] is as follows,

$$2^{2^{n+1}-2} \prod_{j=1}^{2^n-1} \sin^2\left(\frac{j}{2^{n+1}}\pi\right) = 2^n, \quad (5)$$

where  $n$  is the logarithmic of the dimension of the Cartan matrix. Note that each sine square term on the equation is actually the eigenvalue  $\lambda_j$  of matrix  $A$ . So the reciprocal of one eigenvalue equals to the product of all the other eigenvalues.

However, Eq. (5) cannot be used directly to inverse the eigenvalues because the number of terms equals to the dimension of the linear system of equations, namely exponential with  $n$ . By exploiting the distribution characteristics of the terms, Eq. (5) can be simplified to

$$\frac{8}{\lambda_j} = \left[ \left(\sin \frac{\pi}{6}\right)^m \prod_{k=2}^{n-m} \sin\left(\frac{|2^k - 2^{-m} j \bmod 2^{k+1}|}{2^{k+1}}\pi\right) \right]^2, \quad (6)$$

where  $n > 2$ , and  $m$  is an integer belonging to  $[0, n-2]$  used to make  $2^{-m}j$  to be an odd

number. Details about the derivation of the equation are described in appendix A. Now the reciprocal of eigenvalues can be regarded as the product of  $2(n-1)$  sine values.

Each sine value of Eq. (6) is prepared on the probability amplitude easily through controlled  $R_y$  rotation. So the amplitude  $1/\lambda_j$  in the solution state can be prepared by implementing the probability amplitude directly. There are no phase estimation, Hamiltonian simulation and arithmetic in the algorithm. The gate-complexity is low and the solution error comes only from the initial discretizing process of the Poisson equation.

### 3. QUANTUM ALGORITHM AND CIRCUIT DESIGN

Our algorithm consists of three stages: basis conversion, inverting the eigenvalues on the probability amplitudes, and uncomputing the basis conversion. The overall circuit is shown in Fig. 1.

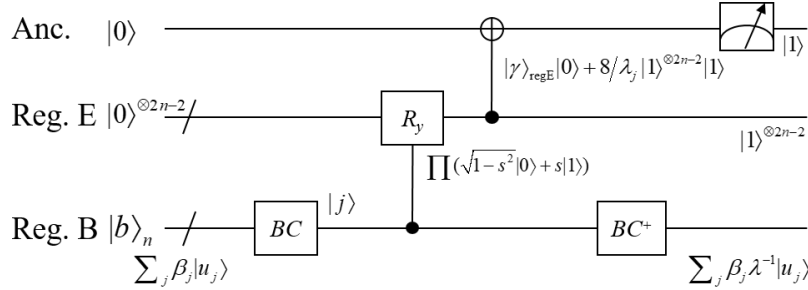


Fig. 1 The overall circuit of our QPS.  $BC$  denotes the basis conversion for converting the basis from  $|u_j\rangle$  to computational basis  $|j\rangle$ . The controlled  $R_y$  rotation and NOT operations are used to inverse the eigenvalues on the probability amplitudes where  $s$  denotes the sine values  $\sin(j\pi/2^{n+1})$ . It is assumed that  $|b\rangle_n = \sum_{i=1}^{2^n-1} b_i |i\rangle$  has been prepared and stored in register B.

By and large, the main produces of our algorithm goes as follows:

- (1) The state  $|b\rangle_n$  in register B can be expressed as  $\sum_{j=1}^{2^n-1} \beta_j |u_j\rangle$  using the eigenstates of matrix  $A$ . The basis is converted into computational basis by  $BC$  circuit as  $BC \cdot |b\rangle_n = \sum_{j=1}^{2^n-1} \beta_j |j\rangle$ .
- (2) The sine values  $\sin(j\pi/2^{n+1})$  is prepared as the probability amplitudes of register E using controlled  $R_y$  rotations. After this step, the computational bases  $|j\rangle$  are entangled with the  $2(n-1)$  sine terms on the right hand side of Eq. (6).
- (3) The state of  $C/\lambda_j |1\rangle$  on the ancillary qubit are prepared using the controlled NOT operation controlled by the  $2(n-1)$  sine terms in register E.
- (4) Uncompute the basis conversion in register B. After this step, the eigenstates  $|u_j\rangle$

are entangled with the state of ancillary qubit  $C/\lambda_j|1\rangle$ .

- (5) Finally, we measure the state of ancillary qubit. If the measurement is  $|1\rangle$ , then the state in register B is  $\sum_j \beta_j \lambda_j^{-1} |u_j\rangle$  which represents the solution of the Poisson equation. The variable time amplitude amplification technique [28] can be applied before measurement to increase the success probability of obtaining the solution.

### 3.1 Basis conversion

The initial state of register B can be expressed as  $|b\rangle_n = \sum_{j=1}^{2^n-1} b_j |j\rangle = \sum_{j=1}^{2^n-1} \beta_j |u_j\rangle$  using the computational basis  $|j\rangle$  and eigenstates  $|u_j\rangle$  of matrix  $A$ , respectively. A unitary operator  $U$  is required to accomplish the following transform,

$$U|u_j\rangle = |j\rangle. \quad (7)$$

That is, the  $j^{\text{th}}$  row of the operator  $U$  is  $u_j$ ,

$$U = [u_1, u_2, \dots, u_{2^n-1}]^T. \quad (8)$$

Apparently,  $U$  is the sine transform [16,29]. More specifically, we can design the basis conversion circuit by the discrete sine transform (DST) of type I in Ref. [29]. The DST is related to discrete Fourier transform (DFT) as follows,

$$T_N^\dagger FT_{2N} T_N = C_{N+1}^I \oplus (-iS_{N-1}^I). \quad (9)$$

The  $T_N$  is a basis change matrix, and the  $FT_{2N}$ ,  $C_{N+1}^I$  and  $S_{N-1}^I$  represents the transform of Fourier, cosine and sine, respectively. The sine transform  $S_{N-1}^I$  can be implemented using Eq. (9) as shown in Fig. 2. Details about this circuit can be found in Ref. [18].

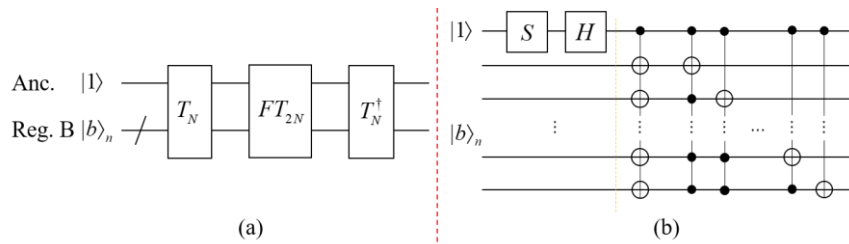


Fig. 2 The overall circuit for sine transform (a), and for transform  $T_N$  (b). The ancillary qubit is set to be  $|1\rangle$  used to pick out sine transform in Eq. (9). The circuit costs  $n$  qubits and  $O(n^2)$  elementary gates [30].

### 3.2 Inversing the eigenvalues

The reciprocal of eigenvalues are calculated using Eq. (6). The sine terms are indexed by two variables, namely  $m$  and  $k$ . So the circuit to inverse the eigenvalues contains two

levels. For the first level, the circuit consists of  $n-1$  modules, as shown in Fig. 3, which corresponds to  $m$  being from 0 to  $n-2$ . Note that in each module  $2^{-m}j$  is an odd number.

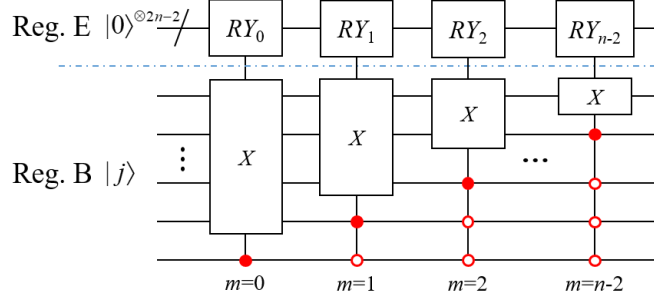


Fig. 3 The overall circuit to calculate the reciprocal of eigenvalues. In general, the circuit consists of  $(n-1)$  controlled  $RY$  modules numbered with  $m$  from 0 to  $n-2$ . Each  $RY$  module is controlled by two kinds of control qubits called global and local control qubits. The global control qubits are the lower  $(m+1)$  qubits in Reg. B which are represented by the red dots and circles. The global control qubits are actually used to pick out such  $j$  that  $2^{-m}j$  is an odd number. The local ones are the higher  $(n-m)$  qubits of Reg. B inside the  $X$  modules which are described below. Note that the  $(n-1)$   $RY$  modules are computed serially. They can turn to be parallel by adding  $n-2$  ancillary qubits, and then the depth of the circuit is reduced from  $O(n^3)$  to  $O(n^2)$ , see appendix B for a feasible design.

The second level is the controlled  $RY_m$  module which actually implements Eq. (6) with the corresponding  $m$ . Each  $RY$  module contains  $n-1$  terms of square of sine values. The sine values can be prepared as probability amplitudes easily using the  $R_y$  rotation. And the square of sine values can be obtained using two qubits as follows,

$$R_y^{\otimes 2}(2\theta)|0\rangle^{\otimes 2} = \cos^2 \theta|00\rangle + \cos \theta \sin \theta|01\rangle + \sin \theta \cos \theta|10\rangle + \sin^2 \theta|11\rangle. \quad (10)$$

Fig. 4 shows the circuit design for the controlled  $RY_0$  and  $RY_1$  modules.

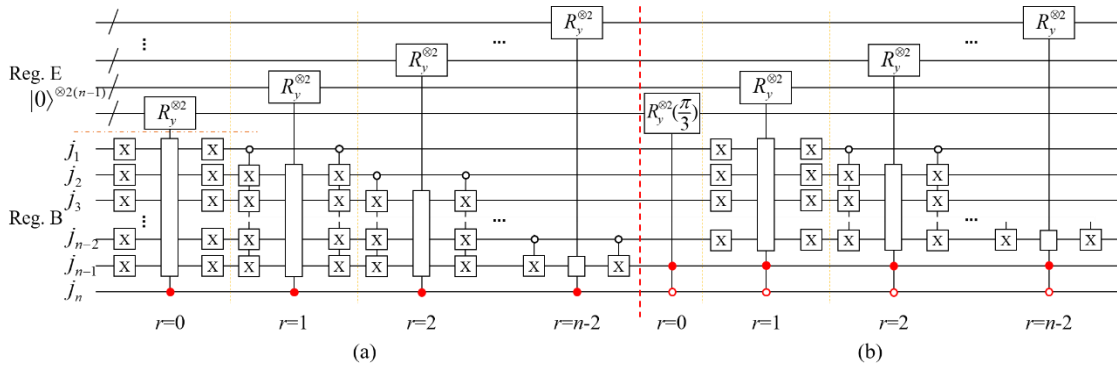


Fig. 4 The circuit design for  $RY_0$  module (a), and  $RY_1$  module (b). Each  $RY$  module consists of  $n-1$  terms of square of sine values. Each  $R_y^{\otimes 2}$  operator produce one sine square. The  $R_y^{\otimes 2}$  modules are indexed by  $r$ . For  $r$  from 0 to  $m-1$ , it is to produce the constant terms of  $\sin^2(\pi/6)$ ; and for  $r$  from  $m$  to  $n-2$ , it is to produce the terms that  $k$  being from  $n-m$  down to 2. The  $NOT$  gates are used to calculate the complements of  $j$ .

The circuit to implement the controlled  $R_y^{\otimes 2}$  operation is rather simple as shown in Fig. 5. For a state  $|j\rangle$  in register B, the binary representation can be written as

$$j = j_1 j_2 \cdots j_n = \sum_{k=1}^n 2^{n-k} j_k. \text{ Then the } R_y \text{ rotation can be expressed as}$$

$$R_y\left(\frac{j\pi}{2^n}\right) = e^{-i\frac{j\pi}{2^{n+1}}Y} = e^{-i\frac{\pi}{2^{n+1}}\left(\sum_{k=1}^n 2^{n-k} j_k\right)Y} = \prod_{k=1}^n e^{(-i\frac{2^{n-k}\pi}{2^{n+1}}Y)j_k} = \prod_{k=1}^n R_y^{j_k}\left(\frac{\pi}{2^k}\right), \quad (11)$$

where  $j_k$  is the local control qubit. Fig. 5 is designed based on this equation by adding the global control qubit.

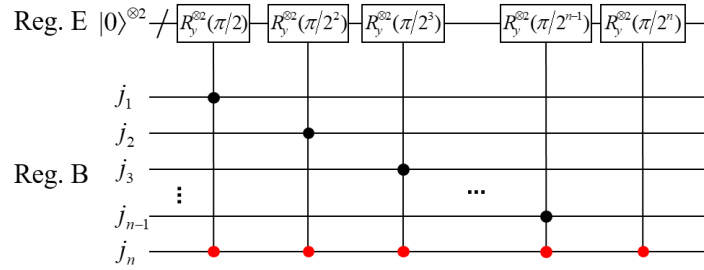


Fig. 5 The circuit for the first  $R_y^{\otimes 2}$  operation in  $RY_0$  module in Fig. 4. The black dots are the local control qubits.  $j_n$  is both global and local control qubit. According to Lemma 6.1 in ref. [30], one  $R_y^{\otimes 2}$  controlled by 2 qubits can be decomposed into 8 two-qubit gates.

The state evolution during the produce of inverting the eigenvalues can be expressed as follows,

$$|0\rangle^{\otimes 2n-2} \sum_{j=1}^{2^n-1} \beta_j |j\rangle \rightarrow \sum_{j=1}^{2^n-1} \beta_j \left[ \left( \cos \frac{\pi}{6} |0\rangle + \sin \frac{\pi}{6} |1\rangle \right)^m \prod_{k=2}^{n-m} (\sqrt{1-s^2} |0\rangle + s |1\rangle) \right]^{\otimes 2} |j\rangle, \quad (12)$$

where  $s = \sin\left(\frac{|2^k - 2^{-m} j \bmod 2^{k+1}|}{2^{k+1}} \pi\right)$ . As can be seen from the equation, the probability

amplitude of the state  $|1\rangle^{\otimes 2n-2}$  in register E is the same as that of the solution state as shown in Eq. (6). In order to pick out the state  $|1\rangle^{\otimes 2n-2}$  in register E, a controlled *NOT* operation executed on an ancillary qubit is used as shown in Fig. 1. After this operation, the state evolves into

$$\sum_{j=1}^{2^n-1} \beta_j \left[ |\gamma\rangle_{\text{regE}} |0\rangle + 8/\lambda_j |1\rangle^{\otimes 2n-2} |1\rangle \right] |j\rangle, \quad (13)$$

where  $|\gamma\rangle$  is an unnormalized state representing all the other states in register E except

$|1\rangle^{\otimes 2n-2}$ .

Finally, the basis conversion is uncomputed and the system state evolves into

$$\sum_{j=1}^{2^n-1} \beta_j \left[ |\gamma\rangle_{\text{regE}} |0\rangle + 8/\lambda_j |1\rangle^{\otimes 2n-2} |1\rangle \right] |u_j\rangle. \quad (14)$$

Before the measurement, the variable time amplitude amplification technique can be used to increase the success probability of obtaining the solution. If the measurement result of the Ancillary qubit in Fig. 1 is  $|1\rangle$ , then the system state collapses into  $|1\rangle^{\otimes 2n-2} |1\rangle \sum_j \beta_j \lambda_j^{-1} |u_j\rangle$ . Therefore, the solution state is created in register B.

#### 4. GATE-COMPLEXITY, DEPTH AND ERROR ANALYSIS

Now we analyze the complexity, depth and error of our algorithm. As can be seen from Fig. 1, the present algorithm needs  $3n$  qubits, where  $n=\log N$  and  $N-1$  is the dimension of the linear system of equations. Considering the ancillary qubits, the least number of qubits required is  $3n+1$  [30]. In general, we can add less than  $n$  ancillary qubits to reduce the complexity of decomposition of gates.

For the gate-complexity, the total number of gates required is  $5/3n^3$  in one- and two-qubit gates. Furthermore, if the multi-controlled one-qubit and one-controlled multi-qubit gates can be applied, like the new methodologies of  $i$ -Toffoli/CNOT <sup>$n$</sup>  operations [31], the number of gates required can be reduced sharply.

The depth of our QPS mainly depends on the way of implementing the controlled  $R_y$  rotation as shown in Fig. 1. If the  $R_y$  modules are executed serially as shown in Fig. 3, the depth of the circuit is  $5/3n^3$ . After parallelizing the  $R_y$  modules as discussed in appendix B, the depth is reduced to  $10n^2$ . This improvement is achieved by simply adding another  $n-2$  ancillary qubits.

Since the cost of our circuit is small and the depth can be shallow, the present QPS has the potential to solve a non-trivial problem on NISQ devices. For example, if solving the one-dimensional Poisson equation by discretizing it with  $2^{15}$  points, our QPS can be implemented using 46 qubits and tens of thousands of elementary gates. After parallelization, the depth of the QPS circuit is several thousand with a need of 60 qubits. This cost is acceptable for the NISQ devices with fidelity of 99.99% [32]. The output state encodes the solutions of more than 32 thousand points into the probability amplitudes.

Throughout our algorithm, the operations related to eigenvalues are performed on the probability amplitude, which induces no errors as that in phase estimation and arithmetic. Therefore, the solution error of our algorithm comes only from the finite difference approximation of the Poisson equation. As mentioned above, the truncation error is  $\varepsilon=1/N^2$ . Considering  $n=\log N$ , we have  $n=1/2\log(1/\varepsilon)$ . So the complexity of our algorithm is  $\log(1/\varepsilon)$  in qubits and  $\text{poly}(\log(1/\varepsilon))$  in quantum operations. Such performance of the complexity on the error is consistent with the best known result [5-7]. Additionally, any direct or iterative classical algorithms for solving the Poisson equation with error  $\varepsilon$  have a cost of at least  $\varepsilon^{-\alpha}$ , where  $\alpha > 0$  is a smoothness constant [33]. So our algorithm offers an exponential speedup over classical method in terms of error.

## 5. DEMONSTRATION

We demonstrate our algorithm on a quantum virtual computing system installed on the Sunway TaihuLight Supercomputer in Wuxi, China [34]. Comparing with Eq. (6), Eq. (5) is a more direct way of calculating the reciprocal of eigenvalues, but it has exponential number of terms. Fig. 6 (a) and (b) show the circuits for the case of  $n=2$  corresponding to Eq. (5) and (6), respectively. Circuit (a) costs 12 qubits and 130 one- and two-qubit gates. In comparison, (b) costs just 6 qubits and 90 gates. The number of qubits used in register E is  $2(2^2-1)$  and  $2(2-1)$ , respectively. It is an exponential reduction. With further optimizations, e.g. simplifying the *QFT* [35] in basis conversion, the cost of the circuit can be reduced.

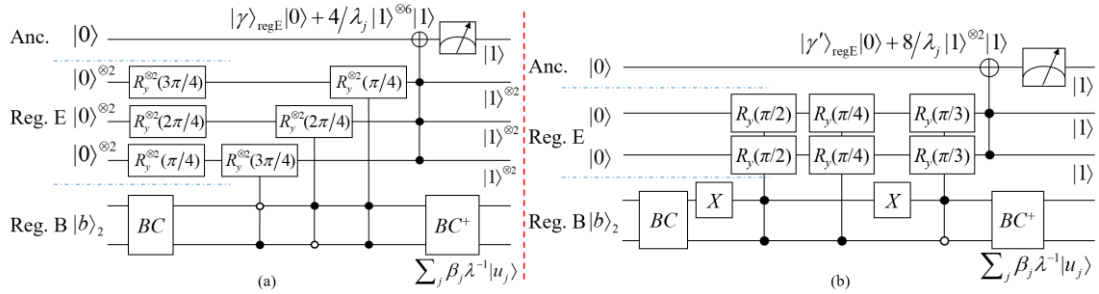


Fig. 6 The circuits for the case of  $n=2$  using two schemes to inverse the eigenvalues, (a) based on Eq. (5), and (b) Eq. (6).

The state of  $|b\rangle_2$  is initialized as  $1/\sqrt{2}|01\rangle + 1/2|10\rangle + 1/2|11\rangle$ . The result of the circuit executed on the virtual system is  $[0.552987, 0.674065, 0.489736]^T$  after normalized, while the expected result calculated using python is  $[0.552988, 0.674065, 0.489736]^T$ . The difference between them is less than  $2^{-21}$ . The effectiveness of circuit (b) can be verified on state-of-the-art quantum hardware [26].

## 6. CONCLUSIONS

We present a compact quantum Poisson solver (QPS) for solving the one-dimensional Poisson equation. Through the algorithm, the major operations related to eigenvalues are performed on probability amplitudes by single-qubit  $R_y$  rotation. The expensive procedures of phase estimation, Hamiltonian simulation and quantum arithmetic can be circumvented. The solution error comes only from the finite difference approximation of the Poisson equation. The idea of executing function calculations on probability amplitude by single-qubit rotation should be inspirational in many ways for optimizing quantum algorithms.

The costs of our QPS is nearly optimal, that is,  $3n$  in qubits and  $5/3n^3$  in one- and two-qubit gates, where  $n$  is the logarithmic of the dimension of the linear system of equations. And the dependence of the gate-complexity on solution error is  $\log(1/\epsilon)$  in qubits and  $\text{poly}(\log(1/\epsilon))$  in quantum operations, which consists with the best known results and achieves an exponential speedup over classical method. When solving the

Poisson equation by discretizing it into  $2^{15}$  points, our algorithm needs only 46 qubits and tens of thousands of one- and two-qubit gates. The solution error is, in theory,  $2^{-30}$ . So the present QPS should be capable of running on Noisy Intermediate-Scale Quantum (NISQ) devices.

An open question is how to extend the present algorithm to  $d$ -dimensional Poisson equation. For higher dimensions, the eigenvalues are the sum of that of one-dimensional case. There should be an intuitive way to inverse the eigenvalues on probability amplitudes, like quantum signal processing [36], and achieve a complexity having nearly linear dependence on  $d$ .

## ACKNOWLEDGEMENTS

We are very grateful to the National Supercomputing Center in Wuxi for the great computing resource. We would also like to thank the technical team from the Origin Quantum Computing Technology co., LTD in Hefei for the professional services on quantum virtual computation. The present work is financially supported by the National Natural Science Foundation of China (Grant No. 61575180, 61701464, 11475160) and the Pilot National Laboratory for Marine Science and Technology (Qingdao).

## APPENDIX A

We use central difference approximation to discretize the one-dimensional Poisson equation, and the resulted linear system of equations is solved by the QLSA. The discretized matrix  $A$  is a Cartan matrix, and the product of all its eigenvalues forms a sine formula as shown in Eq. (5) [22]. This equation shows that the reciprocal of each eigenvalue is equal to the product of the remained  $2^n-2$  eigenvalues. The number of terms can be reduced exponentially as shown in Eq. (6) in the following way.

Firstly, we study the distribution characteristics of the terms on the left hand side of Eq. (A.1) derived from Eq. (5),

$$\prod_{j=1}^{2^n-1} \sin^2\left(\frac{j}{2^{n+1}}\pi\right) = 2^{n+2-2^{n+1}}. \quad (\text{A.1})$$

The angular coefficient  $j/2^{n+1}$  of each term is listed in the way as shown in Fig. A.1. Apparently, each layer contains  $2^{n-1}$  odd terms because  $j$  is an odd number, and  $2^{n-1}-1$  even terms. All of the even terms in one layer are actually the ones of the adjacent upper layer, and each even term always corresponds to an odd one of some upper layer. That is, all the terms of one layer, say  $n=4$  layer, are actually the odd terms of the present and upper layers, i.e. layers of  $n=4, 3, 2, 1$ . So all the terms are divided into  $n$  groups and each group contains only the odd terms of that layer.

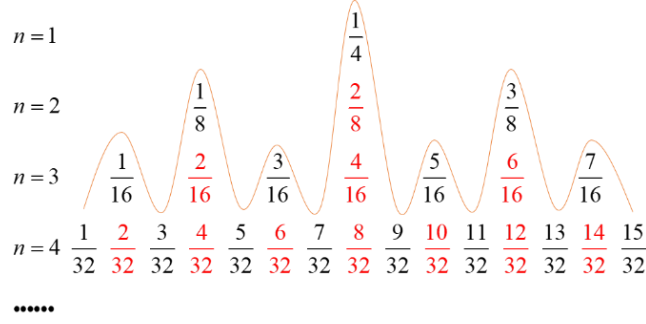


Fig. A.1 The angular coefficient  $j/2^{n+1}$  of each term in Eq. (5) for  $n=1, 2, 3, 4$ . The characteristic of distribution is that the terms of one layer consist of all of the odd terms of the present and upper layers.

Using the distribution characteristics, the product can be re-organized with only the odd terms of each layer as follows,

$$\prod_{k=1}^n \prod_{j=1}^{2^{k-1}} \sin^2 \frac{(2j-1)\pi}{2^{k+1}} = 2^{n+2-2^{n+1}}. \quad (\text{A.2})$$

Secondly, we analyze the reciprocal of each term  $\sin^2(j\pi/2^{n+1})$ . The following discussions are divided into two conditions for  $j$  being an odd number and an even number.

When  $j$  is an odd number belonging to  $[1, 2^n-1]$ , starting from Eq. (A.1) we have

$$\begin{aligned} \sin^{-2}\left(\frac{j}{2^{n+1}}\pi\right) &= 2^{2^{n+1}-n-2} \prod_{\substack{k=1 \\ k \neq j}}^{2^n-1} \sin^2\left(\frac{k}{2^{n+1}}\pi\right) \\ &= 2^{2^{n+1}-n-2} \sin^2\left(\frac{2^n-j}{2^{n+1}}\pi\right) \prod_{\substack{k=1 \\ k \neq j \\ k \neq 2^n-j}}^{2^n-1} \sin^2\left(\frac{k}{2^{n+1}}\pi\right) \\ &= 2^{2^{n+1}-n-2} \sin^2\left(\frac{2^n-j}{2^{n+1}}\pi\right) \sin^2\left(\frac{2^{n-1}}{2^{n+1}}\pi\right) \cdot \prod_{\substack{k=1 \\ k \neq j \\ k \neq 2^n-j}}^{2^{n-1}-1} [\sin^2\left(\frac{k}{2^{n+1}}\pi\right) \sin^2\left(\frac{2^n-k}{2^{n+1}}\pi\right)] \\ &= 2^{2^{n+1}-n-2} \sin^2\left(\frac{2^n-j}{2^{n+1}}\pi\right) \sin^2\left(\frac{2^{n-1}}{2^{n+1}}\pi\right) \cdot \prod_{\substack{k=1 \\ k \neq j \\ k \neq 2^n-j}}^{2^{n-1}-1} [\sin^2\left(\frac{k}{2^{n+1}}\pi\right) \cos^2\left(\frac{k}{2^{n+1}}\pi\right)] \\ &= 2^{2^{n+1}-n-2} \sin^2\left(\frac{2^n-j}{2^{n+1}}\pi\right) \sin^2\left(\frac{2^{n-1}}{2^{n+1}}\pi\right) \cdot 2^{4-2^n} \prod_{\substack{k=1 \\ k \neq j \\ k \neq 2^n-j}}^{2^{n-1}-1} \sin^2\left(\frac{k}{2^n}\pi\right) \\ &\dots\dots \\ &= 2^{2^{n+1}-n-2} \left(\prod_{k=2}^n 2^{4-2^k}\right) \cdot \left[\prod_{k=2}^n \sin^2\left(\frac{2^{k-1}}{2^{k+1}}\pi\right)\right] \cdot \left[\prod_{k=2}^n \sin^2\left(\frac{|2^k - j \bmod 2^{k+1}|}{2^{k+1}}\pi\right)\right] \\ &= 2^{2^{n+1}-1} \cdot \prod_{k=2}^n \sin^2\left(\frac{|2^k - j \bmod 2^{k+1}|}{2^{k+1}}\pi\right). \quad (\text{A.3}) \end{aligned}$$

The above derivation contains a recursive process that cut the number of terms of the product by half utilizing the symmetry of distribution in each layer as shown in Fig. A.1. The two trigonometric formulas, i.e.  $\sin 2\theta = 2\sin\theta\cos\theta$  and  $\sin\theta = \cos(\pi/2-\theta)$ , are used repeatedly in the derivation. So the reciprocal of eigenvalues with  $j$  being an odd

number can be calculated by the  $(n-1)$  terms as follows,

$$\frac{C}{\lambda_j} = \frac{C}{2^{2n+2} \sin^2(j\pi/2^{n+1})} = \frac{C}{2^3} \prod_{k=2}^n \sin^2\left(\frac{|2^k - j \bmod 2^{k+1}|}{2^{k+1}} \pi\right). \quad (\text{A.4})$$

When  $j$  is an even number, it can be transformed to an odd one in some upper layer. Suppose  $j = 2^m i$ , where  $i$  is an odd number and  $m$  is an integer belonging to  $[1, n-2]$ , then the even term  $j$  corresponds to the odd term  $i$  in the upper  $m^{\text{th}}$  layer. In such case,  $\sin^{-2}(j\pi/2^{n+1})$  can be calculated as

$$\sin^{-2}\left(\frac{j}{2^{n+1}} \pi\right) = \sin^{-2}\left(\frac{i}{2^{n-m+1}} \pi\right) = 2^{2(n-m)-1} \cdot \prod_{k=2}^{n-m} \sin^2\left(\frac{|2^k - 2^m j \bmod 2^{k+1}|}{2^{k+1}} \pi\right). \quad (\text{A.5})$$

Eq. (A.3) for odd  $j$  can be seen as a special case of Eq. (A.5) with  $m = 0$ . So the reciprocal of eigenvalues for any  $j$  can be calculated by the following equation,

$$\frac{8}{\lambda_j} = \frac{8}{2^{2n+2} \sin^2(j\pi/2^{n+1})} = 4^{-m} \cdot \prod_{k=2}^{n-m} \sin^2\left(\frac{|2^k - 2^m j \bmod 2^{k+1}|}{2^{k+1}} \pi\right). \quad (\text{A.6})$$

The normalizing constant  $C$  is chosen to be 8 which is the lower bound of eigenvalues when  $n \geq 2$ . After transforming the factor  $4^{-m}$  into a sine form, Eq. (A.6) turns to

$$\frac{8}{\lambda_j} = \left[ \left(\sin \frac{\pi}{6}\right)^m \cdot \prod_{k=2}^{n-m} \sin\left(\frac{|2^k - 2^m j \bmod 2^{k+1}|}{2^{k+1}} \pi\right) \right]^2. \quad (\text{A.7})$$

This is pretty intriguing. The reciprocal of  $8/\lambda_j$  is the product of  $(n-1)$  terms and each term is a square of sine value. The first  $m$  terms are constants, namely  $\sin^2(\pi/6)$ . Put it another way, we can inverse the eigenvalues through  $2(n-1)$  sine terms. The number of terms of the product is reduced exponentially from  $2(2^n-2)$  to  $2(n-1)$ , and this guarantees that the complexity of our algorithm is  $3n$  in qubits.

## APPENDIX B

In Fig. 3, the  $RY$  modules are executed serially. The gate-complexity of the circuit is low, but the depth is high to run efficiently on NISQ devices. Here we propose a feasible way of paralleling the  $RY$  modules to reduce the depth from  $O(n^3)$  to  $O(n^2)$ . The parallelization consists of three aspects as follows.

Firstly, parallelize the control qubits in Fig. 3. One more register  $C$  with  $(n-2)$  qubits is allocated to store the global control qubits. The control qubits are parallelized by the  $CP$  (Control-qubits Parallelization) module as shown in Fig. B.1.

Secondly, break up each  $RY$  module in Fig. 4 into the basic unit of controlled  $R_y^{\otimes 2}$  and assemble new module called  $RYP$  ( $RY$  Parallelization). Let  $R_y(m, r)$  represent the controlled  $R_y^{\otimes 2}$  indexed by  $m$  and  $r$  as shown in Figs. 3 and 4, respectively. The assembling rule is that the  $R_y(0, r)$ ,  $R_y(1, r+1 \bmod (n-1))$ , ...,  $R_y(m, r+m \bmod (n-1))$ , ..., and  $R_y(n-2, r+n-2 \bmod (n-1))$  constitute the module  $RYP_r$ . Fig. B.1 shows the circuit for  $RYP_0$  and  $RYP_1$ . In this way, all the  $R_y^{\otimes 2}$  are rearranged to be parallel in each  $RYP$  module.

Thirdly, as shown in Fig. 5, the controlled  $R_y^{\otimes 2}(\pi/2^i)$  in each  $RYP$  are also rearranged to be parallel. The basic idea is illustrated in Fig. B.2 for  $RYP_0$  module.

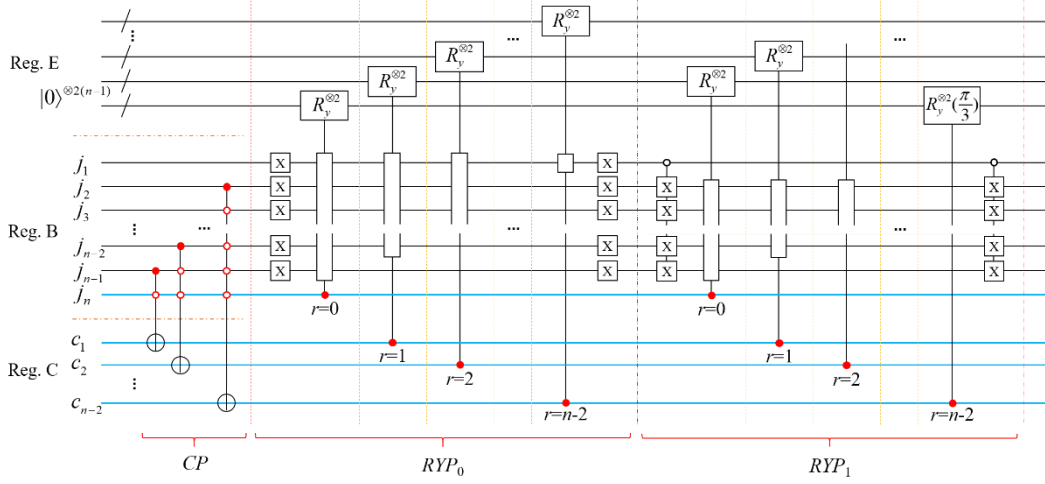


Fig. B.1 A feasible way of parallelizing the  $RY$  modules in Fig. 3. The  $CP$  module is used to parallelize the control qubits and  $RYP$  represent the parallelized  $RY$  modules. The depth of  $CP$  is  $5(n-2)^2$  when the multi-controlled NOT gates are decomposed into one- and two-qubit gates.

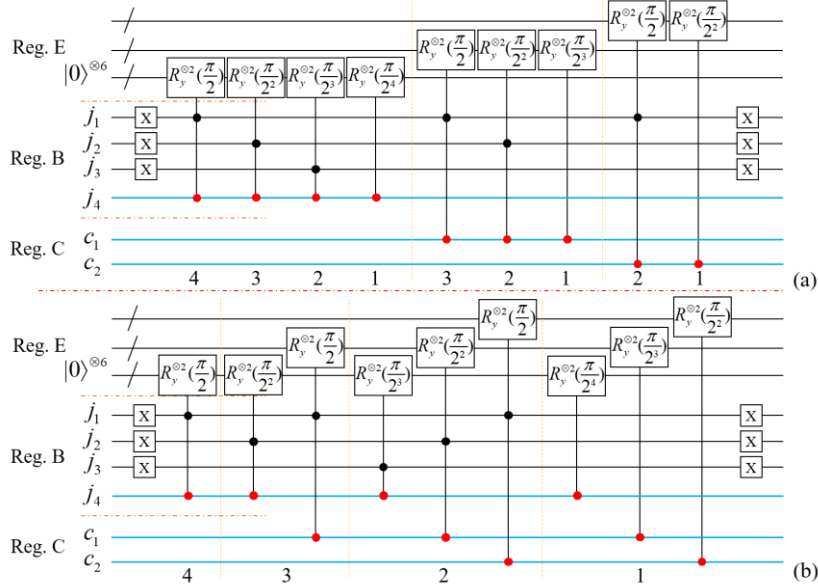


Fig. B.2 The way of parallelizing the controlled  $R_y^{\otimes 2}(\pi/2^i)$  in  $RYP_0$  module with  $n=4$ . (a) The original arrangement, and (b) the re-arrangement. The controlled  $R_y^{\otimes 2}(\pi/2^i)$  with the same number labeled below the circuit in (a) is rearranged together in (b). The depth of the  $RYP_0$  is reduced from  $4n^2$  to  $8n$  when decomposed by one- and two-qubit gates. The numbers imply that the depth of  $RYP$  depends on  $RY_0$ . The total depth of  $RYP$  modules is  $5n^2$ .

As we can see, the depth of our parallel-version QPS mainly depends on the  $RY_0$  and

$CP$  modules. Note that the qubits in register  $E$  can also be used to do the decomposition of multi-qubit gates before  $RYP$  modules, then there is no need to adding more ancillary qubits. Hence, the gate-complexity of  $RY$  modules turns to  $4n$  in qubits and the depth reduces from  $5/3n^3$  to  $10n^2$ . When  $n=15$ , the depth of inverting eigenvalues based on serial and parallel  $RY$  modules is about 8000 and 1800, respectively. Since the decomposition of the multi-controlled one-qubit and one-controlled multi-qubit gates constitutes the major cost, the depth of  $T_N$  in  $BC$  and  $CP$  in  $RY$  can be reduced to  $O(n)$  using the technology of  $i$ Toffoli/CNOT $^n$  gates [31]. Additionally, the depth of  $FT_{2N}$  in  $BC$  can also be reduced to  $O(n)$  even  $O(\log n)$  [37,38].

## REFERENCES

1. Shor, P. W. Algorithms for quantum computation: discrete logarithms and factoring proceedings. *In Proc. 35th Annual Symposium on Foundations of Computer Science*, 124–134 (1994).
2. Montanaro, A. Quantum algorithms: an overview. *npj Quantum inf.* **2**, 15023 (2016).
3. Leyton, S.K. & Osborne, T.J. A quantum algorithm to solve nonlinear differential equations. arXiv: 0812.4423 (2008).
4. Berry, D. W. High-order quantum algorithm for solving linear differential equations. *J. Phys. A: Math. Theor.* **47**, 105301 (2014).
5. Berry, D. W., Childs, A. M., Ostrander, A. & Wang, G. Quantum algorithm for linear differential equations with exponentially improved dependence on precision. *Commun. Math. Phys.* **356**, 1057-1081 (2017).
6. Childs, A.M. & Liu, J. P. Quantum spectral methods for differential equations. arXiv: 1901.00961 (2019).
7. Childs, A.M., Liu, J. P. & Ostrander, A. High-precision quantum algorithms for partial differential equations. arXiv:2002.07868 (2020).
8. Costa, P., Jordan, S. & Ostrander, A. Quantum algorithm for simulating the wave equation. *Phys. Rev. A* **99**, 012323 (2019).
9. Arrazola, J.M., Kalajdziewski, T., Weedbrook, C. & Lloyd, S. Quantum algorithm for nonhomogeneous linear partial differential equations. *Phys. Rev. A* **100**, 032306 (2019).
10. Harrow, A. W., Hassidim, A. & Lloyd, S. Quantum algorithm for linear systems of equations. *Phys. Rev. Lett.* **103**, 150502 (2009).
11. Childs, A. M., Kothari, R. & Somma, R. D. Quantum algorithm for systems of linear equations with exponentially improved dependence on precision. *SIAM J. Comput.* **46**, 1920–1950 (2017).
12. Dervovic, D., Herbster, M., Mountney, P., Severini, S., Usher, N. & Wossnig, L. Quantum linear systems algorithms: a primer. arXiv: 1802.08227 (2018).
13. Berry, D. W., Childs, A. M. & Kothari, R. Hamiltonian simulation with nearly optimal dependence on all parameters. *Proceedings of the 56<sup>th</sup> Annual IEEE Symposium on Foundations of Computer Science*, 792-809 (2015).
14. Kalajdziewski, T. & Arrazola, J. M. Exact gate decompositions for photonic quantum computing. *Phys. Rev. A* **99**, 022341 (2019).
15. Ford, W. Numerical linear algebra with applications: Using MATLAB. *Academic Press* (2014).
16. Cao, Y., Papageorgiou, A., Petras, I., Traub, J. & Kais, S. Quantum algorithm and circuit design

- solving the Poisson equation. *New J. Phys.* **15**, 013021 (2013).
17. Steijl, R. & Barakos, G.N. Parallel evaluation of quantum algorithms for computational fluid dynamics. *Comput. Fluids* **173**, 22-28 (2018).
  18. Wang, S., Wang, Z., Li, W., Fan, L., Wei, Z. & Gu, Y. Quantum fast Poisson solver: the algorithm and complete and modular circuit design. *Quantum Inf. Process.* **19**, 170 (2020).
  19. Bhaskar, M. K., Hadfield, S., Papageorgiou, A. & Petras, I. Quantum Algorithms and circuits for scientific computing. *Quantum Inf. Comput.* **16**, 197–236 (2015).
  20. Häner, T., Roetteler, M. & Svore, K.M. Optimizing quantum circuits for arithmetic. arXiv:1805.12445 (2018).
  21. Wang, S., Wang, Z., Li, W., Fan, L., Cui, G., Wei, Z. & Gu, Y. Quantum circuits design for evaluating transcendental functions based on a function-value binary expansion method. arXiv:2001.00807 (2020).
  22. Damianou, P. A. A beautiful sine formula. *Am. Math. Mon.* **121**, 120-135 (2014).
  23. Tomza, M., Jachymski, K., Gerritsma, R., Negretti, A., Calarco, T., Idziaszek, Z. & Julienne, P. S. Cold hybrid ion-atom systems. *Rev. Mod. Phys.* **91**, 035001 (2019).
  24. Arute, F., Arya, K., Babbush, R. et al. Quantum supremacy using a programmable superconducting processor. *Nature* **574**, 505–510 (2019).
  25. Figgatt, C., Ostrander, A., Linke, N.M. et al. Parallel entangling operations on a universal ion-trap quantum computer. *Nature* **572**, 368–372 (2019).
  26. Krantz, P., Kjaergaard, M., Yan, F., Orlando, T.P., Gustavsson, S. & Oliver, W. D. A quantum engineer’s guide to superconducting qubits. *Appl. Phys. Rev.* **6**, 021318 (2019).
  27. Demmel, J.W. Applied numerical linear algebra. *SIAM, Philadelphia* (1997) chap.6.
  28. Ambainis, A. Variable time amplitude amplification and quantum algorithms for linear algebra problems. *29th Symposium on Theoretical Aspects of Computer Science*, 636–647 (2012).
  29. Klappenecker, A. & Rotteler, M. Discrete cosine transforms on quantum computers. arXiv:quant-ph/0111038 (2001).
  30. Barenco, A., Bennett, C. H., Cleve, R. et al. Elementary gates for quantum computation. *Phys. Rev. A* **52**, 3457–3467 (1995).
  31. Rasmussen, S. E., Groenland, K., Gerritsma, R., Schoutens, K., & Zinner, N. T. Single-step implementation of high fidelity n-bit Toffoli gate. *Phys. Rev. A* **101**, 022308 (2020).
  32. Preskill, J. Quantum Computing in the NISQ era and beyond. *Quantum* **2**, 79 (2018).
  33. Ritter, K. & Wasilkowski, G.W. On the average case complexity of solving Poisson equations. *Lect. Appl. Math.* **32**, 677-688 (1996).
  34. Chen, Z. Y., Zhou, Q., Xue, C., Yang, X., Guo, G. C. & Guo, G. P. 64-qubit quantum circuit simulation. *Sci. Bull.* **63**, 964-971 (2018).
  35. Nam, Y., Su, Y. & Maslov, D. Approximate quantum Fourier transform with  $O(n \log(n))$  T gates. *npj Quantum Inf.* **6**, 26 (2020).
  36. Low, G. H. & Chuang, I. L. Optimal Hamiltonian simulation by quantum signal processing. *Phys. Rev. Lett.* **118**, 10501 (2017).
  37. Cleve, R. & Watrous, J. Fast parallel circuits for the quantum Fourier transform. *Proc. 41st Annual Symposium on Foundations of Computer Science*, 526 (2000).
  38. Maslov, D. Linear depth stabilizer and quantum Fourier transformation circuits with no auxiliary qubits in finite-neighbor quantum architectures. *Phys. Rev. A* **76**, 052310 (2007).